Kinetic study of the liquid-phase hydrogenation of 1-butyne over a commercial palladium/alumina catalyst

J.A. Alves [a,b,c], S.P. Bressa [a,b,d,*], O.M. Martínez [a,b,c], G.F. Barreto [a,b,c]

[a] *Centro de Investigación y Desarrollo en Ciencias Aplicadas, Universidad Nacional de La Plata, Argentina*
[b] *Programa de Investigación y Desarrollo en Reactores Químicos, Facultad de Ingeniería, Universidad Nacional de La Plata, Argentina*
[c] *Consejo Nacional de Investigaciones Científicas y Técnicas, Argentina*
[d] *Comisión de Investigaciones Científicas de la Província de Buenos Aires, Argentina*

Abstract

Hydrorefining of C_4 cuts of unsaturated hydrocarbons involves the selective removal of 1-butyne by catalytic hydrogenation. Due to its technological relevance, we investigated the hydrogenation of 1-butyne over a commercial palladium-based catalyst of the eggshell type. The experimental conditions were selected to reproduce those of industrial hydrorefining reactors: liquid-phase reaction, seven levels of temperature between 27 and 62 °C, initial concentrations of 1-butyne up to 0.6 mol/l and hydrogen partial pressure ranging from 0.8 to 8 atm. Under these conditions, the overall effectiveness factor of 1-butyne hydrogenation was less than 0.15. Provided that hydrogen was the limiting reactant inside the active shell, 1-butene was the only product yielded by 1-butyne hydrogenation. The regression analysis of experimental data corresponding to the hydrogenation of 1-butyne to 1-butene was restricted to experimental compositions in which 1-butyne concentration was higher than 0.07 mol/l. An intrinsic kinetic expression with reaction orders 1 and −1 for hydrogen and 1-butyne, respectively, predicts experimental data with an average deviation of 2.1%. Estimates of the activation energy and kinetic coefficient at 44 °C are $(1.55 \pm 0.06) \, 10^4$ cal/mol and (4.6 ± 0.1) mol/(kg s).
© 2006 Elsevier B.V. All rights reserved.

Keywords: Liquid-phase hydrogenation; 1-Butyne; Pd eggshell catalyst

1. Introduction

Most petrochemical and petroleum refineries include hydrorefining reactors for the upgrading of C_4 cuts of unsaturated hydrocarbons originated in cracking operations. To take advantage of these C_4 cuts as industrial sources of pure 1,3-butadiene, isobutene or *n*-butenes, several hydrorefining operations were developed [1]. In general, the reaction system involves the hydrogenation of 1-butyne and 1,3-butadiene and the hydrogenation and hydroisomerization of the *n*-butenes.

A common target to all C_4 cuts hydrorefining operations is the selective removal of 1-butyne from the cut by catalytic hydrogenation. This reaction takes place before the reactions of the rest of the unsaturated hydrocarbons fed to the hydrorefining reactors. Hence, in this paper we focus our study on the kinetics of the hydrogenation of 1-butyne. The results presented in this paper allowed us to gain knowledge about 1-butyne hydrogenation before dealing with the complete reaction system.

For the purpose of this contribution, it is worthy to highlight the following features of industrial hydrorefining operations [1,2]. Current technologies use catalytic fixed-bed reactors with concurrent flow of hydrocarbons, in liquid state, and hydrogen. Major catalyst manufacturers supply palladium-based catalysts as the standard alternative for hydrorefining reactors. Commercial catalysts are of the eggshell type with palladium content within 0.05–0.5% (w/w). Typical concentrations of 1-butyne in the cut are about 1% molar. Operating temperatures are between 20 and 60 °C. Pressure levels raise up to 10 atm to operate with hydrocarbons in liquid-phase. Under these conditions, the resulting hydrogen partial pressure is about 5 atm.

An extensive investigation was devoted to the vapour-phase hydrogenation/deuteration of 1-butyne over palladium/alumina catalysts [3–7]. Each of these studies was performed at a unique level of temperature, covering all of them the range 0–35 °C. 1-Butyne was always the limiting reactant with hydro-

gen/deuterium to 1-butyne ratios of 2–6. Chief targets of these works were the assessment of metal particle size effects and the identification of product distribution, catalytic mechanisms and surface reactive species. The liquid-phase hydrogenation of 1-butyne over palladium was studied by Boitiaux et al. [8]. Their experiments were done at 20 °C with laboratory catalysts in a powder form. Hydrogen pressure was maintained constant at 20 atm and the initial molar fraction of 1-butyne was 20%. In a latter paper, Boitiaux et al. [9] proposed a mechanistic kinetic expression for the hydrogenation of 1-butyne. This expression is based on the major experimental trends observed in their experiments. Molnár et al. [10] reviewed published studies on catalytic hydrogenation of alkynes. They remarked that most studies focused on the influence of metal dispersion, carbon deposits, promoters and additives on selectivity; whereas kinetic studies aimed at validating kinetic expressions are scarce.

It is concluded that experimental data concerning the behaviour of commercial catalysts under operating conditions of industrial hydrorefining reactors is not available in literature. In addition, the validation of a kinetic expression and the statistical estimation for the corresponding parameters remain to be done. Hence, we performed a kinetic investigation of the hydrogenation of 1-butyne over a palladium/alumina commercial catalyst of the eggshell type. To this end, the experiments were designed to reproduce typical operating conditions of industrial hydrorefining reactors. The kinetic study presented in this contribution allowed us to obtain reliable estimates of the activation energy and of the kinetic coefficient.

2. Experimental

2.1. Catalyst and other materials

The main features of the palladium/alumina commercial catalyst used in this study are listed in Table 1.

1-Butyne (99.0%, Matheson) and 1-butene (99%, Alphagaz) were used after flowing through a bed of 4A molecular sieve (UOP) and a guard bed loaded with the same catalyst as used in the experiments. Hydrogen (99.999%, AGA) and nitrogen (99.998%, AGA) were purified from water and oxygen by passing the stream through a guard bed with the same commercial catalyst followed by a 4A molecular sieve and an oxygen trap (Alltech). *n*-Propane (99.99%, AGA) and *n*-hexane (97% HPLC, Baker) were purified on individual 4A molecular sieves before using them in the experiments.
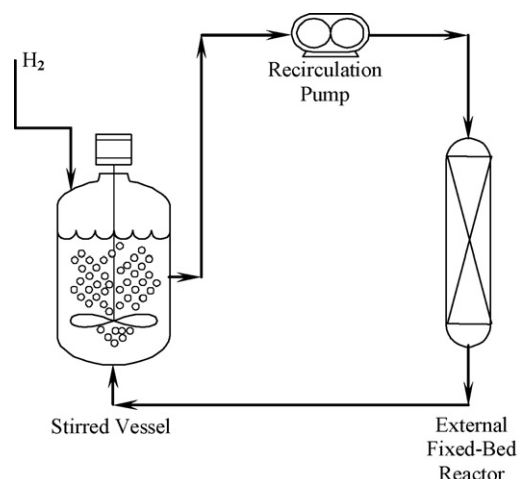

Fig. 1. Recirculation system with an external fixed-bed reactor.

2.2. Experimental set-up and operation

Batch experiments with respect to the unsaturated reactants were performed. The main components of the experimental set-up are sketched in Fig. 1.

The 100-ml stirred vessel (Autoclave Engineers Series 0.75), which contains most of the liquid in the loop, allows temperature control and to maintain the reacting liquid saturated with hydrogen. An electrical heater, connected to a control tower (Autoclave Engineers CT-100), encloses the stirred vessel. The same control tower serves for setting the agitation speed of the impeller, which allows for stirring and dispersing the gas into the liquid. The agitation speed was 2000 rpm. This value proved to be high enough to maintain the liquid saturated with hydrogen at reaction conditions.

A gear micropump magnetically driven (Micropump 200) impulses the reacting mixture downward through the external fixed-bed reactor. The catalyst sample, in its original size, is placed in a stainless steel 1/4-in. tube enclosed in a jacket. Heating water, at the same temperature as the stirred vessel, circulated through the jacket.

The load of known volumes of *n*-hexane as inert solvent allowed to obtain desired values of 1-butyne and 1-butene initial concentrations. In addition, the use of *n*-hexane facilitated the sampling for chromatographic analysis. The initial amounts of 1-butyne and 1-butene were calculated on the basis of the flow rate measured during the loading of each of them.

Table 1
Catalyst features [11]

|			
Shape	Sphere	Mean pore radius	37 ± 6 nm
Type	Eggshell	Active shell thickness	0.24 mm
Diameter	2.5 mm	Porosity (ε)	0.4
Bulk density (ρ_{cat})	1150 kg/m^3	Specific surface area of Pd	0.55 m^2/g$_{activeshell}$
Volumetric fraction of the active shell (f_V)	0.49	Metal particle size	3.6 nm
Pd loading in the catalyst pellet	0.21% (w/w)	Dispersion	27%
Specific surface area (BET)	70 ± 20 m^2/g	Tortuosity factor (τ)	1.5 ± 0.6
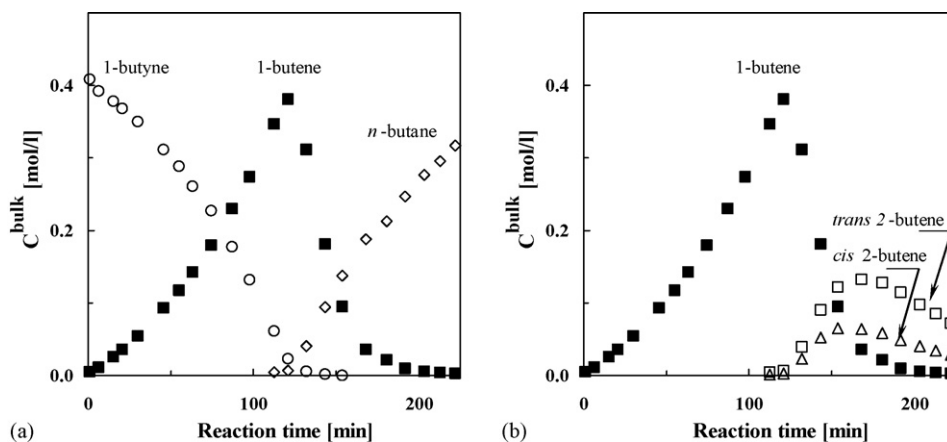
Fig. 2. Variation of hydrocarbons bulk concentrations with reaction time at 44 °C, $p_{H_2} = 2.29$ atm and $M_{cat} = 505.1$ mg.

Total operating pressure was maintained constant by feeding hydrogen through a pressure regulator. Hydrogen partial pressure and total pressure were independently regulated by loading a proper amount of *n*-propane. Thus, hydrogen partial pressure in the stirred vessel, and so the hydrogen mole fraction in the reaction mixture, could be chosen within a wide range and kept constant during each run.

The reacting liquid flows through the fixed-bed reactor at 700 ml/min, which is the maximum rate attainable by the gear micropump. This flow rate was high enough to produce a very low conversion of 1-butyne *per* pass. Therefore, the bulk composition was essentially uniform along the whole system. It was also confirmed that, at 700 ml/min, temperature was uniform throughout the system.

Catalyst samples were treated for reduction finishing in the reactor previously described. Following the manufacturer indications, the catalyst was exposed to an hydrogen/nitrogen (1/3) stream for 9 h at 54 °C.

The hydrocarbons present in the reaction mixture were *n*-propane, *n*-hexane and the C_4 hydrocarbons that take part in the reaction system: 1-butyne, 1-butene, *n*-butane, *cis* and *trans* 2-butene. Hydrocarbon composition was determined from liquid samples analysed by gas chromatography employing a FID detector. To determine the mole fraction of each hydrocarbon, we used two chromatographic columns of 2 m by 2 mm: a VZ-10 60/80 column provided by Alltech operated at 50 °C, and a column packed with 0.19% picric acid on 80–100 mesh Graphpac operated at room temperature. Constancy of hydrogen partial pressure along each run was tested by injecting samples of the vapour-phase to a conductivity cell.

Some others details concerning the experimental system were described in Ref. [12].

3. Experimental results

The ranges of the experimental conditions explored in this study are listed in Table 2.

The evolution of hydrocarbon concentrations in all of the experiments performed with 1-butyne as the only initial C_4 hydrocarbon showed the pattern outlined in Fig. 2.

Table 2
Ranges of experimental conditions

Weight of catalyst samples (M_{cat})	250–1000 mg
Temperature (T)	27–62 °C
Hydrogen partial pressure (p_{H_2})	0.8–8 atm
Initial concentration of 1-butene	0 and 0.7 mol/l (0 and 9% molar basis)
Initial concentration of 1-butyne	0.4–0.6 mol/l (5–8% molar basis)

1-Butene is the only product of reaction formed until 1-butyne reaches a high level of conversion. At longer reaction times, 1-butene neatly reacts to form *n*-butane (Fig. 2a) and *cis* and *trans* 2-butene (Fig. 2b). This pattern clearly indicates that 1-butyne is capable to saturate the catalytic surface, inhibiting the readsorption and, hence, the catalytic reactions of 1-butene. For the most part, the hydrogenation of 1-butyne accelerates, thus showing a negative reaction order which confirms that 1-butyne covers all the active sites.

The inhibition effect of 1-butyne upon 1-butene is also effective at higher 1-butene concentrations, as revealed by the results shown in Fig. 3, corresponding to an experiment with high initial concentration of 1-butene. Again, 1-butene can react only after 1-butyne conversion is very high. It can be inferred that the
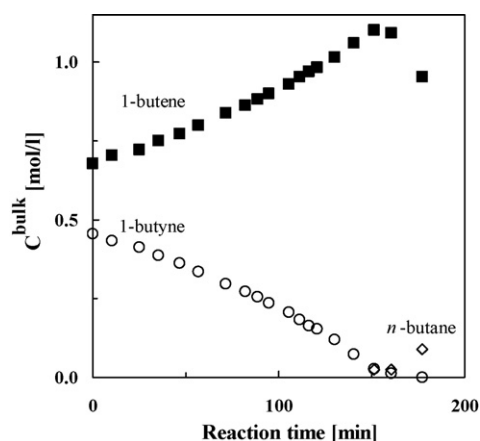

Fig. 3. Variation of 1-butyne, 1-butene and *n*-butane bulk concentrations at 44 °C, $p_{H_2} = 2.51$ atm and $M_{cat} = 494.5$ mg.

catalytic sites active for the hydrogenation of 1-butyne are the same as those for the reactions of 1-butene.

Although 1-butyne concentrations at which 1-butene can react are low, Figs. 2 and 3 show that it is possible to identify a certain 1-butyne concentration level at which 1-butene starts to react. This level is mainly determined by hydrogen partial pressure and not by 1-butene concentration. To understand this behaviour it must be pointed out that the reaction rate is severely limited by mass transport resistances (cf. 5. Results from the regression analysis). This is perhaps rather surprising on account of the thin active shell of the catalyst, but our experiments revealed that the hydrogenation of 1-butyne proceeds strongly restrained by intracatalyst diffusion limitations. Moreover, we found that the transport resistance in the liquid film must be also considered.

The strong diffusion resistance makes the concentration of the limiting reactant, either hydrogen or 1-butyne, become essentially nil inside the active shell. If the limiting reactant inside the active shell is 1-butyne, there will be an hydrogen surplus. In this case, the inner part of the catalytic shell will be depleted from 1-butyne and 1-butene will be capable to adsorb and react with the hydrogen surplus. Therefore, 1-butene can react inside the active shell even if 1-butyne bulk concentration is high enough to inhibit 1-butene reactions in the absence of mass transport limitations. Thus, the reaction times at which the 2-butenes and n-butane appear in Figs. 2 and 3 indicate that 1-butyne became the limiting reactant inside the active shell. Before that reaction time, the absence of the 1-butene reactions indicates that 1-butene was never able to compete with 1-butyne for the active sites.

We will restrict our quantitative analysis to experimental data collected before the production of 2-butenes and n-butane becomes noticeably, i.e. when hydrogen is the limiting reactant. As it will be demonstrated below, this set of experimental data allowed us to obtain accurate estimates of the kinetic coefficient of the hydrogenation of 1-butyne and of the corresponding activation energy.

4. Analysis of experimental data

The available information for each experimental run is the composition in the bulk of the liquid in terms of mole fractions for each hydrocarbon, x_j^{bulk}, at a set of reaction times. Then, C_j^{bulk} values were obtained by multiplication x_j^{bulk} and the total molar concentration of the reacting mixture. We neglected in the treatment the amount of hydrocarbons in the vapour-phase, as this was checked to be less than 1%. Variations of the total molar concentration along each experiment run were less than 0.5% and so it was considered constant. Hydrogen and total concentration were calculated by using the Redlich–Kwong–Soave equation of state modified by Graboski and Daubert for hydrocarbon mixtures containing hydrogen [13].

As the reaction mixture is a dilute solution of reactants in n-hexane, 1-butyne and hydrogen diffusion inside the catalyst were modelled by a Fickean equation with effective diffusion coefficients defined by:

$$D_j^{ef} = \frac{\varepsilon}{\tau} D_j, \tag{1}$$

where D_j denotes the binary molecular diffusion coefficient of "j" in n-hexane, ε the catalyst porosity and τ is the catalyst tortuosity factor. The values of D_j corresponding to the hydrocarbons and hydrogen were estimated by using the equations proposed by Tyn and Calus [14] and by Akgerman and Gainer [15], respectively. As an example, under operating conditions of Figs. 2 and 3 the ratio $D_{H_2}^{ef}/D_{butyne}^{ef}$ is 4.6.

It was previously remarked (cf. Section 2.2) that $x_{H_2}^{bulk}$, and so $C_{H_2}^{bulk}$, was kept constant along each experimental run. Therefore, the following model is based on the fact that $C_{H_2}^{bulk}$ does not vary with the reaction time during the course of each run.

The conservation equation corresponding to 1-butyne during each experimental run is

$$V \frac{dC_{butyne}^{bulk}}{dt} = -M_{cat} r^{obs}, \tag{2}$$

where V is the total volume of the liquid reaction mixture in the closed-loop of Fig. 1, t the time of reaction, M_{cat} the weight of the catalyst sample and r^{obs} is the observed rate of reaction. In writing Eq. (2), it was considered that the catalytic bed operates under uniform composition because of the high recirculation flow rate. In addition, the batch volume was considered constant because the volume of liquid extracted for sampling proved to be negligible.

Instantaneous values of r^{obs} were calculated by using

$$r^{obs} = \eta_i \, r^s, \tag{3}$$

in which η_i is the intracatalyst effectiveness factor for 1-butyne hydrogenation and r^s is the reaction rate of 1-butyne hydrogenation evaluated from composition at the external surface of the catalyst.

Mass transport from the liquid bulk to the external surface of the catalyst is expressed by

$$\kappa_j(C_j^{bulk} - C_j^s) = \left(\frac{L_{shell} \, \rho_{cat}}{f_V} \right) \, r^{obs}, \tag{4}$$

where κ_j is the liquid–solid mass transport coefficient of "j", C_j^s represents the concentration of "j" at the catalyst external surface, L_{shell} the thickness of the active shell, f_V the volumetric fraction of the active shell and ρ_{cat} is the catalyst density. The correlation proposed by Gunn [16] was used to estimate κ_j.

Recalling that severe diffusion limitations operates within the active shell, the formalism developed by Aris [17] leads to the following expression to evaluate η_i from instantaneous values of C_j^s,

$$\eta_i = \frac{\sqrt{I}}{h}. \tag{5}$$

In Eq. (5) h is the Thiele modulus defined as

$$h = L_{shell} \sqrt{\frac{(\rho_{cat}/f_V) r^s}{D_{H_2}^{ef} C_{H_2}^s}}. \tag{6}$$

In defining h and in expressing Eq. (4), it was considered that the active shell is thin enough to ignore the curvature effect.
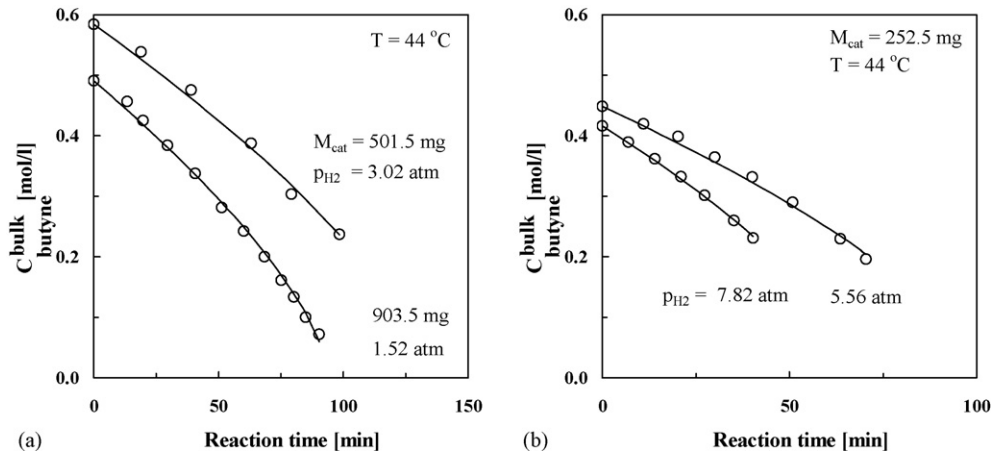
Fig. 4. Influence of hydrogen partial pressure.

The factor I in Eq. (5) is defined as

$$I = 2\frac{\int_0^{C_{H_2}^s} r \; dC_{H_2}}{r^s \; C_{H_2}^s},$$ (7)

where r and C_{H_2} hold for the intracatalyst values of reaction rates and hydrogen concentrations. In defining Eq. (7), it was taken into account that hydrogen is the limiting reactant inside the active shell.

The overall effectiveness factor, η, was also computed according to

$$\eta = \frac{r^s}{r^{bulk}}\eta_i,$$ (8)

where r^{bulk} is the reaction rate of 1-butyne evaluated from the bulk composition.

The software Athena Visual Workbench 8.3 [18] was used to solve the differential and algebraic model (2–7) and to perform the regression analysis in the nonlinear single-response bayesian estimation mode.

5. Results from the regression analysis

An exploratory regression analysis, based only on experimental data collected at 44 °C, was performed. To this end, we employed the following power-law kinetic expression

$$r = k\frac{(C_{H_2})^m}{(C_{butyne})^n}.$$ (9)

This regression analysis proved that Eq. (9) predicts experimental data with an average deviation of 2.4% with $m = 0.92 \pm 0.05$ and $n = 1.11 \pm 0.08$. Therefore, we employed the kinetic expression

$$r = k\frac{C_{H_2}}{C_{butyne}}$$ (10)

to perform the regression analysis of the whole database.

To avoid the strong correlation between the Arrhenius constants we used the following expression to estimate the dependence of temperature on the kinetic coefficient [19]:

$$k(T) = k(T_{ref}) \; \exp\left[\frac{-E_a}{R}\left(\frac{1}{T} - \frac{1}{T_{ref}}\right)\right],$$ (11)
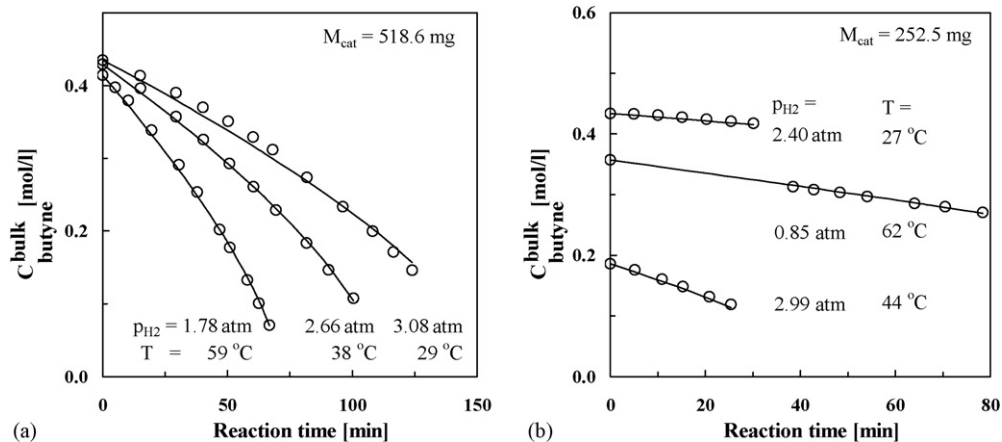

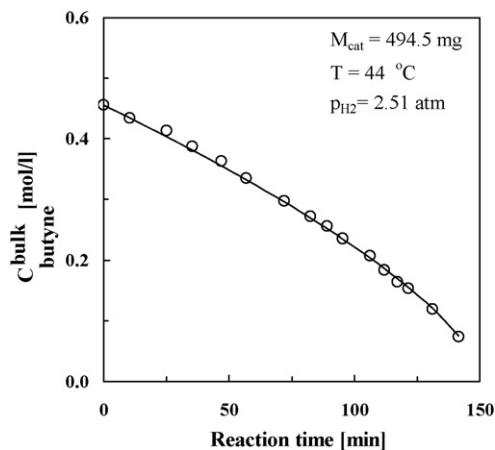Fig. 5. Influence of temperature and hydrogen partial pressure.

Fig. 6. 1-Butyne hydrogenation in presence of 1-butene as initial reactant (cf. Fig. 3).

where T holds for temperature, T_{ref} is 317 K (44 °C), E_a the activation energy and R is the ideal-gas law constant.

A visual comparison between experimental results and their estimates predicted by the model, represented by symbols and lines, respectively is shown in Figs. 4–6. Results plotted in these figures cover the entire range of temperature and composition explored in our study.

The average deviation over the 154 observations collected from 18 experimental runs is 2.1%. The parity-plot presented in Fig. 7 shows that no systematic deviations are noticeable between all the experimental and predicted 1-butyne concentrations.

Optimal estimates of the kinetic parameters are $k(T_{ref}) = (4.6 \pm 0.1)$ mol/(kg$_{cat}$ s) and $E_a = (1.55 \pm 0.06) \times 10^4$ cal/mol.

In consideration of the loss of sensitivity caused by the diffusion limitations, the precision of parameter estimates is quite satisfactory. Precision of model predictions indicates the very good homogeneity of the catalyst samples and reproducibility of the experimental protocol.

The overall effectiveness factor was always less than 0.15. The contribution of the liquid film resistance to the overall effec-
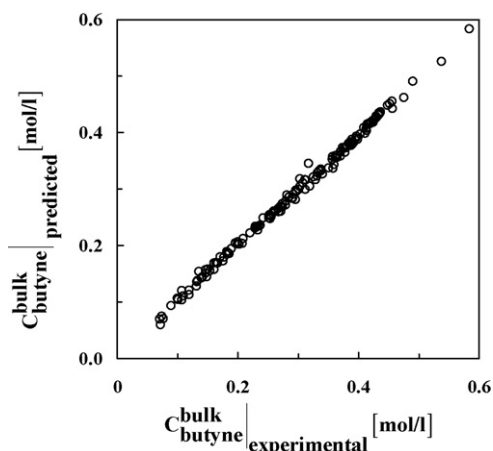
tiveness factor increases with increasing levels of temperature and of the ratio $C_{H_2}^{bulk}/C_{butyne}^{bulk}$. Thus, the most significant influence of liquid film resistance was found at the end-point of the experimental run performed at 59 °C and $p_{H_2} = 1.78$ atm shown in Fig. 5a. In this case, the resulting values of η and η_i were 0.013 and 0.017, respectively. The low values of η_i obtained in all of the experiments informed in this paper, validate the use of Eq. (5).

6. Outline of mechanisms proposed in the literature for 1-butyne hydrogenation over palladium catalysts

The purpose of the following outline consists in giving support to the kinetic expression Eq. (10). However, it must be borne in mind that the validation of a kinetic model does not imply the validation of the mechanism from which it was derived.

It is widely accepted in literature that the major path in the hydrogenation of 1-butyne over palladium involves two elementary steps [3–5,9]. In the first step, an hydrogen adatom is added to the adsorbed 1-butyne to yield a semihydrogenated radical, which reacts with a second hydrogen adatom to form 1-butene in the second step. However, alternative hypothesis were postulated about the source of surface 1-butyne and hydrogen adatoms.
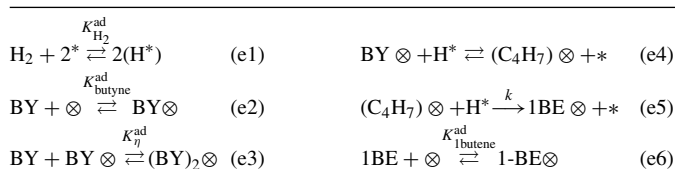
We will assume that there is no competition between hydrogen and 1-butyne for the same active sites. Also, it will be assumed that hydrogen adatoms originate from dissociative adsorption of hydrogen molecules. Both assumptions were validated for the hydrogenation of 1,3-butadiene [20] and for the hydrogenation and hydroisomerization of the *n*-butenes [11] over palladium-based catalysts.

Meyer and Burwell [3] proposed a reaction mechanism that involves the adsorption of 1-butyne with the opening of one π-bond to form a σ-diadsorbed superficial intermediate. Bond and Wells [4] posed a mechanism that proceeds from π-adsorbed 1-butyne bonded to two active sites. Hub and Touroude [5] and Boitiaux et al. [9] postulated that a 1-butyne π-intermediate adsorbed on one metal site is in equilibrium with a more stable complex consisting of one metal site and two molecules of 1-butyne. The active intermediate is the π-adsorbed 1-butyne, whereas the stable complex remains inactive. We also considered in this study a mechanism that admits the coexistence on the catalytic surface of σ-diadsorbed and π-monoadsorbed 1-butyne intermediates, but only the latter is responsible for the formation of the semihydrogenated radical. This scenario was proposed for the hydrogenation of ethene [7].

We have derived the kinetic expressions corresponding to each of the mechanisms outlined above. The kinetic expression derived from the proposal of Hub and Touroude [5] and Boitiaux et al. [9], which leads to the mechanism described in Table 3, is the only one able to represent a negative order with respect to 1-butyne.

In Table 3 we assumed that the elementary steps (e1)–(e4) and (e6) are fast and that the inhibition terms of hydrogen are negligible. Furthermore, we assumed that the fraction of sites $\otimes$ covered by the semihydrogenated radical, (C$_4$H$_7$)$\otimes$, is negligible. Under these assumptions, the following kinetic expression

Fig. 7. Predicted vs. experimental values of C_{butyne}^{bulk}.

Table 3
Catalytic mechanism for 1-butyne hydrogenation

$$H_2 + 2^* \underset{}{\overset{K^{ad}_{H_2}}{\rightleftarrows}} 2(H^*) \quad (e1) \qquad BY \otimes + H^* \rightleftarrows (C_4H_7) \otimes + * \quad (e4)$$

$$BY + \otimes \underset{}{\overset{K^{ad}_{butyne}}{\rightleftarrows}} BY\otimes \quad (e2) \qquad (C_4H_7)\otimes + H^* \overset{k}{\longrightarrow} 1BE \otimes + * \quad (e5)$$

$$BY + BY\otimes \underset{}{\overset{K^{ad}_{\eta}}{\rightleftarrows}} (BY)_2\otimes \quad (e3) \qquad 1BE + \otimes \underset{}{\overset{K^{ad}_{1butene}}{\rightleftarrows}} 1\text{-}BE\otimes \quad (e6)$$

BY: 1-butyne, 1BE: 1-butene, */$\otimes$: sites active for hydrogen/hydrocarbon adsorption.

was obtained:

$$r = \frac{k\, K^{ad}_{butyne}\, C_{butyne}\, C_{H_2}}{1 + K^{ad}_{butyne}\, C_{butyne}(1 + K^{ad}_{\eta}\, C_{butyne}) + K^{ad}_{1butene}\, C_{1butene}}, \quad (12)$$

Experimental conditions included in the regression analysis, presented in the previous section, verify that the catalytic surface is fully covered by 1-butyne surface species. Thus, the inhibition function in Eq. (12) results equal to $K^{ad}_{butyne} C_{butyne}(1 + K^{ad}_{\eta} C_{butyne})$. If the unreactive surface complex $(BY)_2\otimes$ is so strongly adsorbed that $K^{ad}_{\eta} C_{butyne} \gg K^{ad}_{butyne} C_{butyne} \gg 1$, then the expression Eq. (12) becomes

$$r = \left[\frac{k}{K^{ad}_{\eta}} \right] \frac{C_{H_2}}{C_{butyne}}, \quad (13)$$

which shows the same reaction orders as Eq. (10) does.

7. Conclusions

We studied the liquid-phase hydrogenation of 1-butyne over a commercial palladium-based catalyst of the eggshell type. Experimental conditions were close to operating conditions of industrial hydrorefining reactors.

The regression analysis involved experimental data collected during the hydrogenation of 1-butyne until it becomes the limiting reactant inside the active shell. Within this period, 1-butyne is able to inhibit the readsorption and reaction of 1-butene and the only reaction taking place is the hydrogenation of 1-butyne to 1-butene.

A mechanistic kinetic expression is proposed to represent these data, which shows reaction orders equal to -1 and 1 with respect to 1-butyne and hydrogen.

The proposed kinetic expression fits the experimental data with a precision of 2.1%. The kinetic coefficient at 44 °C and the activation energy were estimated with relative precision levels of $\pm 2.1\%$ and $\pm 3.8\%$, respectively.

Overall effectiveness factor values less than 0.15 indicates that the observed reaction rates are strongly affected by mass transport limitations, mainly due to intracatalyst diffusion. The contribution of the liquid film resistance to the overall effectiveness factor was also significant although it was much less important than the contribution of intracatalyst diffusion limitations.

Recalling that hydrorefining of C$_4$ cuts involves the selective removal of 1-butyne from the cut, the strong diffusion limitations evidenced in our experiments would severely impair the selectivity of the industrial operation and, also, increase the catalyst loading. With regard to process selectivity, it can be envisaged that the hydrogen partial pressure is a crucial operating variable whereas temperature level would not pose a significant effect. The presence of hydrogen in excess to the amount required to deplete 1-butyne inside the active shell will activate the hydrogenation reactions of the rest of the unsaturated hydrocarbons present in the cut.

References

[1] M.L. Derrien, Selective hydrogenation applied to the refining of petrochemical raw materials produced by steam cracking, Stud. Surf. Sci. Catal. 27 (1986) 613–666.

[2] R. McClung, S. Novalany, Choosing a selective hydrogenation system, Petrochem. Gas Process. (Autumn) (2002) 147–155.

[3] E.F. Meyer, R.L. Burwell, The reaction between deuterium and 1-butyne, 1,2-butadiene and 1,3-butadiene on palladium-on-alumina catalyst, J. Am. Chem. Soc. 85 (1963) 2881–2887.

[4] G.C. Bond, P.B. Wells, The mechanism of the hydrogenation of unsaturated hydrocarbons on transition metal catalysts, Adv. Catal. 15 (1963) 91–226.

[5] S. Hub, R. Touroude, Mechanism of catalytic hydrogenation of but-1-yne on palladium, J. Catal. 114 (1988) 411–421.

[6] S. Hub, L. Hilaire, R. Touroude, Hydrogenation of but-1-yne and but-1-ene on palladium catalysts. Particle size effect, Appl. Catal. 36 (1988) 307–322.

[7] Ph. Maetz, R. Touroude, Modification of surface reactivity by adsorbed species on supported palladium and platinum catalysts during the selective hydrogenation of but-1-yne, Appl. Catal. A-Gen. 149 (1997) 189–206.

[8] J.P. Boitiaux, J. Cosyns, S. Vasudevan, Hydrogenation of highly unsaturated hydrocarbons over highly dispersed palladium catalyst. Part I: Behaviour of small metal particles, Appl. Catal. 6 (1983) 41–51.

[9] J.P. Boitiaux, J. Cosyns, E. Robert, Hydrogenation of unsaturated hydrocarbons on palladium, platinum and rhodium catalysts. Part I: Kinetic study of 1-butene, 1,3-butadiene and 1-butyne hydrogenation on platinum, Appl. Catal. 32 (1987) 145–168.

[10] Á. Molnár, A. Sarkány, M. Varga, Hydrogenation of carbon–carbon multiple bonds: chemo-, regio- and stereo-selectivity, J. Mol. Catal. A-Chem. 173 (2001) 185–221.

[11] S.P. Bressa, O.M. Martínez, G.F. Barreto, Kinetic study of the hydrogenation and hydroisomerization of the n-butenes on a commercial palladium/alumina catalyst, Ind. Eng. Chem. Res. 42 (2003) 2081–2092.

[12] N.O. Ardiaca, S.P. Bressa, J.A. Alves, O.M. Martínez, G.F. Barreto, Experimental procedure for kinetic studies on egg-shell catalysts. The case of liquid-phase hydrogenation of 1,3-butadiene and n-butenes on commercial Pd catalysts, Catal. Today 64 (2001) 205–215.

[13] M. Graboski, T. Daubert, A modified soave equation of state for phase equilibrium calculations systems containing hydrogen, Ind. Eng. Chem. Process Des. Dev. 18 (1979) 300–306.

[14] M.T. Tyn, W.F. Callus, Diffusion coefficients in dilute binary liquid mixtures, J. Chem. Eng. Data 20 (1975) 106–109.

[15] A. Akgerman, J.L. Gainer, Diffusion of gases in liquids, Ind. Eng. Chem. Fundam. 11 (1972) 373–379.

[16] D.J. Gunn, Transfer of heat or mass to particles, Int. J. Heat Mass Transfer 21 (1978) 467–476.

[17] R. Aris, Elementary Chemical Reactor Analysis, Prentice-Hall, Englewood Cliffs, New Jersey, 1969.

[18] Athena Visual Workbench 8.3, Stewart and Associates Engineering Software, Inc. Available at www.athenavisual.com.

[19] G.E.P. Box, Fitting empirical data, Ann. N.Y. Acad. Sci. 86 (1960) 792–816.

[20] N.O. Ardiaca, S.P. Bressa, J.A. Alves, O.M. Martínez, G.F. Barreto, Kinetic study of the liquid-phase hydrogenation of 1,3-butadiene and *n*-butenes on a commercial Pd/Al$_2$O$_3$ catalyst, Stud. Surf. Sci. Catal. 133 (2001) 527–534.